Indian Journal of Pure & Applied Physics
Vol. 60, August 2022, pp. 627-633
DOI: 10.56042/ijpap.v60i8.64020

An Experimental Evaluation of Quenched Fe-Ga Alloys: Structural Magnetic and Magnetostrictive Properties

V Vijayanarayanan[a], Himalay Basumatary[b], M Manivel Raja[b] & M Mahendran[a*]

[a]Smart Materials Laboratory, Department of Physics, Thiagarajar College of Engineering, Madurai, 625 015 India

[b]Defence Metallurgical Research Laboratory, Kanchanbagh, Hyderabad, 500 058 India

Received 28 June 2022; accepted 18 July 2022

This study examines the effect of quenching on Fe_{100-x}-Ga_x (x – 20 & 25) alloys. The long range of $D0_3$ ordering causes a minor variation in unit cell, which reduces peak intensity. This existence of $D0_3$, coupled with the A2 phase, leads to a decrease in magnetostriction in the quenched 25 at.% Ga alloy, which promotes $D0_3$ ordering. An Fe-Ga alloy having 20 at.% Ga that has been quenched possesses the A2 phase, the production of $D0_3$ is a first-order transition. Continuous ordering attempts to suppress $D0_3$ in 25 at. % Ga alloys were ineffective. Quenched Fe_{80}-Ga_{20} alloy's saturation magnetization is larger than Fe_{75}-Ga_{25} alloy. This suggests that lowering the nonmagnetic element Ga promotes saturation magnetization. The rise in material flaws and dislocations is due to the increased Ga content and higher quenching temperature. In a single-phase region, Fe_{80}-Ga_{20} has the greatest magnetostriction at 85 ppm. Magnetostriction diminishes as Ga content rises to 25%, the $D0_3$ structure is responsible for this drop.

Keywords: Magnetostriction; Galfenol; Phase Transition; Quenching

1 Introduction

Galfenol alloys are a class of functional materials in which magnetic and crystal structures interact when exposed to a magnetic field. Galfenol alloys are a substitute for Terfenol-D alloys, which are rich in rare earth elements but have poor mechanical properties[1]. Due to the effective combination of mechanical and functional qualities of Fe-Ga alloys, galfenol is widely used in sonars, sensors, and actuators. The finest functional qualities are obtained in Fe-Ga alloys with a Ga concentration of 19–27%[2]. Improved functional and mechanical qualities are a result of processing conditions and compositions. Simultaneously, these features of Fe-Ga alloys can be enhanced with the addition of rare-earth elements. Anisotropic deformation happens in the crystal lattice as a result of the atom's magnetic moment being oriented in the direction of the applied magnetic field. Due to their unique features[3], Fe-Ga alloys surpass piezoelectric and Terfenol-D in a variety of applications. Due to the Fe-Ga alloy's high tensile strength and ductility, they can be used in torque sensors, sonar, and actuator applications[4].

Numerous studies have demonstrated that the magnetostriction of Fe considerably increases when nonmagnetic Ga is replaced by Fe. Due to the excellent combination of the aforementioned qualities, Fe_{100-x}-Ga_x (x = 15-30) is hence ideally suited for transducer and actuator applications[5]. With appropriate additions of Ga, the magnetostriction of annealed and quenched $Fe_{80.9}$-$Ga_{19.1}$ increases from 40 to 400 ppm for pure Fe. A few hypotheses have been presented as to the cause of this significant growth, which is not known. Larger magnetostriction in Fe-Ga alloys is mostly dependent on their composition[6]. Clark *et al*. have studied the large magnetostriction of Fe-Ga alloys with Ga contents ranging from 0 to 35%[7].The magnetostriction of higher Fe concentration is significantly enhanced by annealing and quenching, as compared to slow cooling.

Dy and Tb atoms have significant orbital moments, which contribute to the anisotropic magnetostriction of Fe-Ga alloys. Experimental evidence indicates that the addition and substitution of rare earth elements into Fe-Ga alloys increases the saturation magnetostriction[8]. Tb and Dy alloys appear to have a stronger magnetostriction and superior mechanical characteristics in rare earth doped Fe-Ga alloys[9]. Magnetostriction in a material is caused by spin-orbit coupling, which results in the material's magneto crystalline anisotropy[10]. The relevance of anisotropy in magnetostriction was initially recognised when

*Corresponding authors: (Email: perialangulam@gmail.com)

substantial magnetostriction at low temperatures was discovered in rare earth elements such as Tb and Dy, which have a high degree of anisotropy[11]. A large basal plane strain (1%) has been observed in these materials, which is vastly greater than that of ferromagnetic transition metals such as Fe, Co, and Ni.

However, due to the rare earth's low magnetic ordering temperature, the magnetostrictive capabilities could not be used in any application[12]. The dearth of demand for some rare earth metals as a result of their increased use in industrial applications. We need to develop additional substitutes for these rare earth elements by altering compositions and different types of heat treatment. In the case of a polycrystalline Fe-Ga alloy subjected to various heat treatments, the knowledge of ordered and disordered phase formation and their involvement in magnetostriction can vary[13]. The ordered and disordered phase evolution and their effect on the magnetostrictive performance of a quenched polycrystalline bulk Fe-Ga alloy must be investigated because the Fe-Ga alloy displays promise as a material for future actuator applications.

As a result, we have suggested this work to investigate the functional aspects of Fe-Ga alloys with different compositions. In previous reports related to slow cooled Fe_{100-x}-Ga_x (x – 20,15) alloys produced increase in magnetostriction with more addition of Ga[14,15]. We have studied the magnetic, magnetostrictive and structural properties of quenched Fe_{100-x}-Ga_x (x – 20,15) alloys. The ease and simplicity of the quenching process in comparison to other heat treatment techniques is the primary factor in its selection. Quenching also has the added benefit of increasing the metal's endurance and tensile strength. The prepared alloys have A2 and $D0_3$ phases (Fig.1), and the phase structures are based on the alloying and temperatures at which the quenching processes take place. This proves that our quenched Fe-Ga alloys is a prime candidate for sensor and actuator applications.

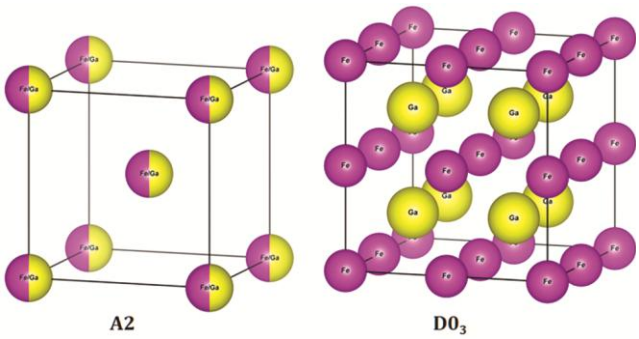

Fig. 1 — A2 and $D0_3$ crystal structures of Fe-Ga alloys.

2 Experimental Conditions

Using Vacuum Arc Melting, Fe-Ga alloys with nominal compositions of 20, 25 at. % Ga were melted. To maintain homogeneity, the prepared alloys were melted and re-melted three times. The alloys were quenched for 4 hours at 950 °C. In order to undertake further characterizations, the alloys were sliced using an EDM wire cutter and an isomet cutter. Grazing-Incidence X-Ray Diffraction, abbreviated as GI-XRD, was used in order to ascertain their structural properties. The microstructure of Fe-Ga alloys was analysed by means of a technique known as scanning electron microscopy (SEM). At room temperature, a Vibrating Sample Magnetometer (VSM) was used to measure the magnetization, and a magnetic field and temperature-compensated resistance strain gauge were used to measure the magnetostriction.

3 Results and Discussions

3.1 Structural Properties

GI-XRD patterns of Fe_{80}-Ga_{20} and Fe_{75}-Ga_{25} alloys quenched at 950 ^oC for 4 hrs is shown in Fig. 2. Four main peaks (110), (200), (211) and (220) are indexed, (110) planes seems to have higher intensity than the other peaks. The peak intensity of the Fe-Ga alloy with higher Fe concentration is higher. The Fe-Ga alloys with lower Ga compositions have lesser peak intensity indicates that the non-magnetic Ga is responsible for this phenomenon. The decrement of peak intensity in higher Ga compositions are due to the attributes of $D0_3$. The higher Fe composition alloy is mostly enriched by BCC A2 phase, but same traces

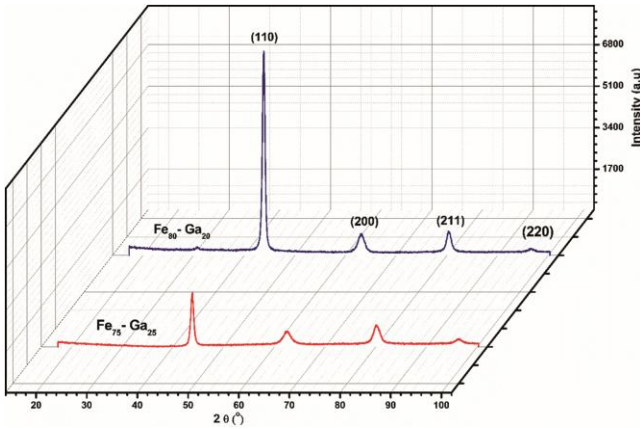

Fig. 2 — GI-XRD patterns of Fe-Ga alloys quenched at 950 ^oC for 4 hrs.

of $D0_3$ and B2 phases are found. But the existence of other particular phase is not known clearly because the alloys below 19 at.% of Ga are pure A2 phase[16]. The existence of other phases are slightly found from the alloy 20 at.% of Ga. The long range ordering of $D0_3$ leads to the small change in unit cell which leads to the decrement of peak intensity. The quenched Fe-Ga alloy containing 20 at.% Ga demonstrates the presence of a single phase A2. Initially, this alloy does not exhibit any ordering during ageing; nevertheless, following quenching, the alloy exhibits $D0_3$ type ordering together with an A2 phase. The presence of the $D0_3$ phase is also observed in a Fe-Ga alloy containing 25% Ga that has been quenched, and the level of $D0_3$ ordering rises with ageing. This existence of $D0_3$, along with the A2 phase, correlates to a decrease in magnetostriction in the quenched Fe-Ga alloy with 25 at.% Ga, which increases the $D0_3$ ordering.

3.2 Surface Morphology

Fig. 3 (a) & (b) shows the micrographs of the Fe-20 & 25 at.% Ga alloys after they have been quenched at 950 ^{o}C for 4 hrs. The alloy with Fe and 20 at.% Ga that has been quenched has the A2 phase, which normally does not undergo any transformations. However, quenching causes the ordered $D0_3$ phase to occur. Furthermore, the microstructure of the slow cooled Fe-20 at.% Ga alloy, which shows the presence of the $D0_3$ phase, supports the metastable phase diagram. The alloy of Fe-25 at.% Ga that has been quenched comprises A2 in addition to the ordered $D0_3$ phase. The metastable phase diagram[14] appears to be followed by the phase formation that occurs during the quenching process, as indicated by the microstructural features that were identified in this work. In the case of alloys containing 20 at.% Ga, the creation of $D0_3$ is a first order transformation[17]. As a result, it takes place as a result of nucleation and growth through a mechanism that is controlled by diffusion. As a consequence of this, there was a possibility that the creation of the $D0_3$ phase could be inhibited during the quenching process[18]. On the other hand, for alloy containing 25 at.% Ga, the A2 phase goes through two stages of sequential continuous ordering: A2 and $D0_3$. Due to the fact that continuous ordering is a faster process, attempts to suppress the development of $D0_3$ in the instance of 25 at.% Ga alloys were unsuccessful.

3.3 Magnetic Properties

The saturation magnetization of Fe_{80} - Ga_{20} and Fe_{75} - Ga_{25} alloys quenched at 950 ^{o}C for 4 hrs is shown in the Fig.4. As with slow cooled alloys, the saturation magnetization of quenched Fe_{80}-Ga_{20} alloy is greater than that of Fe_{75}-Ga_{25} alloy[15]. This indicates that decreasing the nonmagnetic element Ga increases saturation magnetization. Comparing hysteresis with diffraction pattern the higher saturation magnetization and peak intensity at 20 at.% of Ga alloy is due to high enrich A2 phase. The ideal $D0_3$ structure at Fe_{75}-Ga_{25} alloy with long range order is responsible for less magnetization and peak intensity in diffraction pattern. Due to the quenching process and increased Ga content, the coercivity (H_C) and remanent magnetization (M_r) of Fe_{75}-Ga_{25} alloy are greater. The surge in the material defects and dislocations is a result of the increased Ga concentration and higher quenching temperature. These two elements lead to the rise in coercivity[19]. The dM/dH vs H curve shown in Fig.5 was analysed to find how the exchange interactions

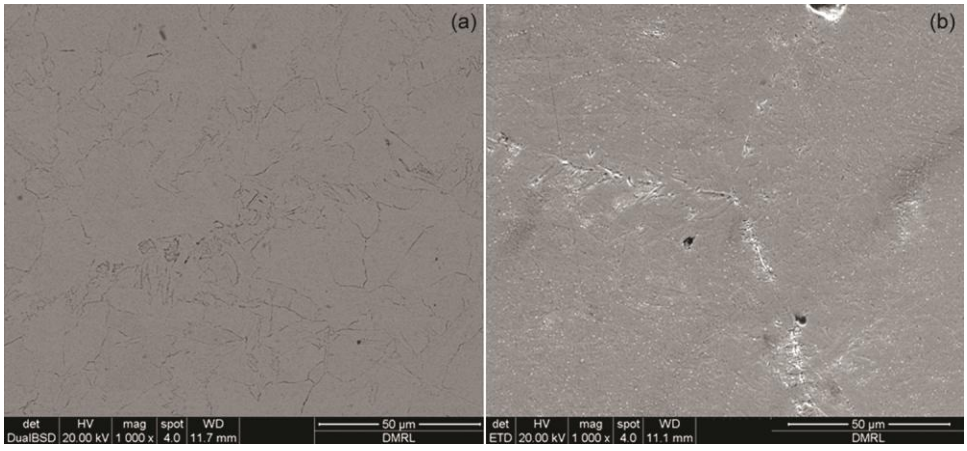

Fig. 3 — SEM micrographs of Fe-Ga alloys quenched at 950 ^{o}C for 4 hrs, (a) Fe_{80}-Ga_{20} and (b) Fe_{75}-Ga_{25}.

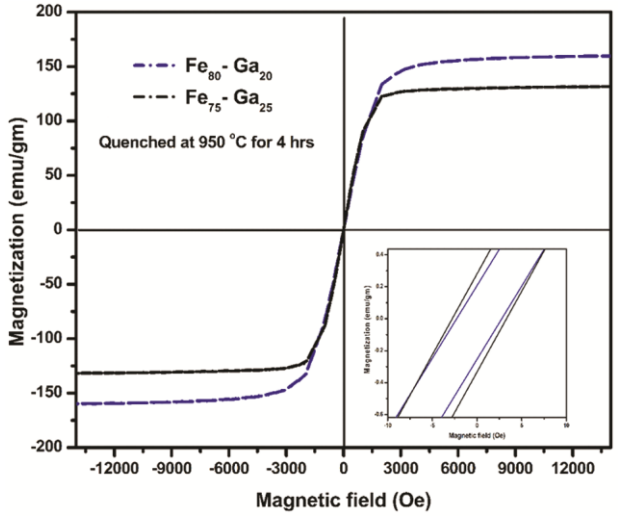

Fig. 4 — Saturation Magnetization of Fe-Ga alloys quenched at 950 °C for 4 hrs.

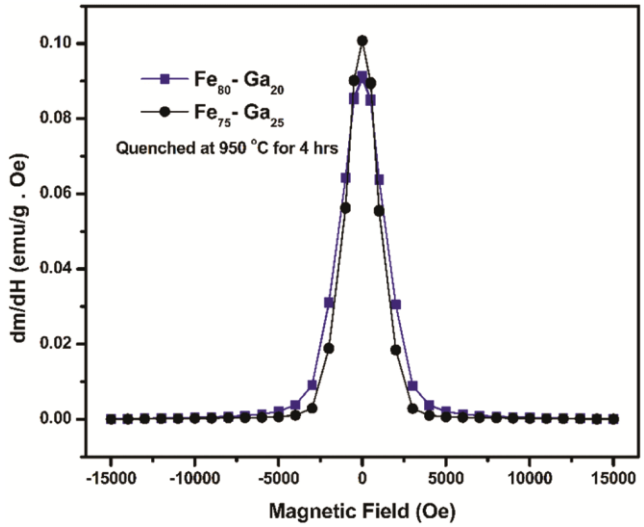

Fig. 5 — The dm/dH vs H curve of Fe-Ga alloys quenched at 950 °C for 4 hrs.

affect the magnetic feature of the quenched Fe -Ga alloys. The maxima peak found in Fe_{75}-Ga_{25} alloy is due to the rise of excellent exchange-coupling. The narrower dm/dH peak reveals good exchange-coupling behaviour. The sharp and higher peak signifies that both phases (A2 and $D0_3$) are parallelly aligned to each other. At higher Fe concentrations (Fe_{80}-Ga_{20}), the peak intensity is reduced, which implies weaker exchange coupling between the phases. Typically, the exchange interaction favours ferromagnetic characteristics. In this case, the remanent magnetization is increased by the exchange interaction between neighbouring pairs (Fe-Fe) that are in different crystallographic directions[20].

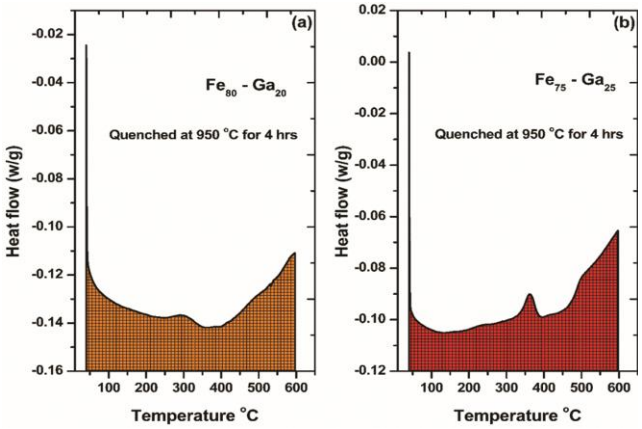

Fig. 6 (a) & (b) — Differential Scanning Calorimetry curve of Fe-Ga alloys quenched at 950 °C for 4 hrs.

3.4 Thermal Properties

Fig. 6 (a) & (b) illustrate the thermal characteristics of Fe_{100}-Ga_{-x} alloys (x – 20 & 25) quenched at 950 °C for 4 hours. The small steepness of the curve at 350 °C in Fig. 6 (a) indicates that the alloy mainly consists of the A2 phase and that the existence of additional phases, such as $D0_3$, begins at this particular composition[21]. In Fe-20Ga alloy, the presence of $D0_3$ and B2 phases is probable. However, the dominating condition of the A2 phase is accountable for the increased saturation magnetization and magnetostriction. In Fig. 6(b), the mountain peak at 350 °C indicates that the $D0_3$ phase is concentrated in this alloy. Even though coercivity (H_C) and remanent magnetization (M_r) are higher in Fe-25Ga alloy, the DSC curve rapidly grows as an exothermic curve beyond 475 °C[22]. It is hypothesised that the A2 phase is ordering and producing the $D0_3$ phase, resulting in a Curie temperature that is substantially lower than average. The A2 phase bcc is fast converting into the $D0_3$ phase in a structure with a mixed phase[16]. When comparing the thermal and magnetostrictive properties of the Fe-Ga alloys the enriched $D0_3$ phase decreases the magnetostrictive property.

3.5 Magnetostrictive Properties

The saturation magnetostriction of Fe_{80}-Ga_{20} and Fe_{75}-Ga_{25} alloys quenched at 950 °C for 4 hrs is shown in Fig.7. Typically, the magnetostriction of Fe-Ga alloys is extremely sensitive to quench annealing at compositions nearer to the order-disorder transition between $D0_3$ and the A2 structure. Also, these quenched samples have a larger saturation magnetostriction at high Fe concentration (Fe_{80}-Ga_{20}) because Ga-Ga couples cause a large amount of atomic strain[23]. When compared to an alloy with the

same composition that has been slow cooled, the magnetostriction of a quenched Fe_{80}-Ga_{20} alloy has a greater value. On the other hand, the saturation magnetostriction of a quenched Fe_{75}-Ga_{25} alloy is lower when compared to the saturation magnetostriction of an alloy with the same composition that was slow cooled[15]. A decrease in saturation magnetostriction occurs as a direct consequence of the creation of the ordered $D0_3$ phase. In the event that the single-phase region is quenched, the highest value is 85 ppm when the Ga content is 20 %. However, as the percentage of Ga in the material increases, up to 25%, magnetostriction decreases to 75 ppm. This decline can be attributed to the organisation that manifests itself as the $D0_3$ structure[24]. The magnetostriction is higher due to dominant A2 phase and the magnetostriction decreases when $D0_3$ phase co-exists with A2. The decrease in magnetostriction in the mixed phase field regime is owing to non-coordinated response of the magnetic domains to the applied field, which is attributed to different phases present in the microstructure[15]. According to prior research, the spin-orbit coupling has a significant role in the magnetostriction and magnetocrystalline anisotropy of Fe-Ga alloys. Assuming that the local magnetocrystalline anisotropy caused by pairs of Ga–Ga improves the magnetostriction behaviour of pure Fe by a large amount when Fe is replaced by non-magnetic Ga, we can say that the large magnetostriction in Fe_{80}-Ga_{20} alloy is caused by quenching, which makes the local magnetocrystalline anisotropy even stronger [25].

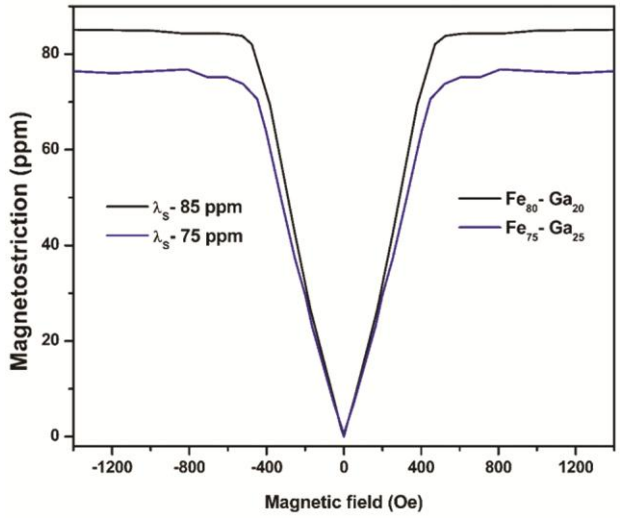

Fig. 7 — Saturation magnetostriction of Fe-Ga alloys quenched at 950 ^oC for 4 hrs.

Table.1 shows the assessment of the magnetostrictive properties of Fe-Ga alloys with different elements. This clearly indicates that the alloying of rare earth elements has higher magnetostriction than conventional Fe-Ga alloys and transition metal doped Fe-Ga alloys. The directional solidification method produces higher magnetostriction than other preparation methods.

Table.1 — Assessment of the magnetostrictive properties of several Fe-Ga alloys.

Preparation Method	Alloy	References	Magnetostriction (ppm)
Arc Melting	Fe_{75}-Ga_{25}	Current work	75
Arc Melting	Fe_{83}-Ga_{17-x}-$Dy_{x-0.2}$	Wang *et al.*[26]	64
Directional solidification	Fe_{81}-Ga_{19-x}-$Tb_{x-0.3}$	Fitchorov *et al.*[27]	112
Induction Melting	Fe_{73}-Ga_{27}	Junming Gou *et al.*[28]	65
Induction Melting	Fe_{83}-Ga_{17-x}-$Cr_{x-0.3}$	Xuexu Gao *et al.*[29]	70
Induction Melting	Fe_{83}-Ga_{17}	LI Jiheng *et al.*[8]	40
Arc Melting	Fe_{73}-Ga_{18}-Zn_9	Yin-Chih Lin *et al.*[30]	33
Arc Melting	Fe_{81}-Ga_{19-x}-$Ge_{x-0.3}$	Fang Gao *et al.*[31]	40
Arc Melting	Fe_{80}-Ga_{20}	K. Perduta *et al*[32]	70
Induction Melting	Fe_{83}-Ga_{17-x}-B_{x-1}	Xuexu Gao *et al.*[29]	50
Arc Melting	Fe_{80}-Ga_{20}	V. Vijayanarayanan *et al*[15]	63
Arc Melting	Fe_{75}-Ga_{25}	V. Vijayanarayanan *et al*[15]	71
Arc Melting	Fe_{80}-Ga_{20}	Sato *et al.*[33]	80
Arc Melting	Fe_{83}-Ga_{17}	Wang *et al.*[26]	40
Rapid solidification	Fe_{85}-Ga_{10}-Al_5	C. Bormio *et al*[34]	75
Arc Melting	Fe_{73}-Ga_{19-x}-Ni_{x-8}	Yin-Chih Lin *et al.*[35]	20
Arc Melting	Fe_{81}-Ga_{19-x}-NBC_{x-1}	A. Sun *et al.*[36]	63
Induction Melting	Fe_{83}-Ga_{17-x}-Y_{x-1}	LI Jiheng *et al.*[8]	55
Arc Melting	Fe_{80}-Ga_{20}	Current work	85

Previous works has also proved that addition of more amount of Ga enhances the magnetostriction in slow cooled Fe-Ga alloys[15]. The results presented in this study proves that our quenched Fe-Ga alloys produces better results than the slow cooled alloys. Galfenol alloys doped with NBC, Ni, Zn, Cr and B has lower saturation magnetostriction. The Fe-Ga alloys, which will be the emerging material for actuators, presents a significant number of practical obstacles and, as a result, a significant number of opportunities for study. The findings that were reported in this study indicate that the A2 and $D0_3$ phases play a significant role in the magnetostrictive properties. These kinds of investigations will be helpful for the research community as they attempt to mould Fe-Ga alloys for usage in the real world.

4 Conclusion

The existence of other phases is slightly found in Fe_{80}-Ga_{20}. The long range of $D0_3$ ordering leads to the small change in unit cell which leads to the decrement of peak intensity. This existence of $D0_3$, along with the A2 phase, correlates to a decrease in magnetostriction in the quenched Fe_{75}-Ga_{25} alloy. An Fe-Ga alloy with 20 at.% Ga that has been quenched has the A2 phase, which normally does not undergo any transformations. However, quenching causes the ordered $D0_3$ phase to occur. In the case of alloys containing 20 at.% Ga, the creation of $D0_3$ is a first order transformation. Due to the fact that continuous ordering is a faster process, attempts to suppress $D0_3$ in the instance of 25 at.%. Ga alloy were unsuccessful. As with slow cooled alloy, the saturation magnetization of quenched Fe_{80}-Ga_{20} alloy is greater than that of Fe_{75}-Ga_{25} alloy. This indicates that decreasing the nonmagnetic element Ga increases saturation Magnetization. The surge in the material defects and dislocations is a result of the increased Ga concentration and higher quenching temperature. Quenched samples have larger saturation magnetostriction at high Fe concentration because Ga-Ga pairs cause a large amount of atomic strain. In the event that the single-phase region is quenched, the highest value is 85 ppm when the Ga content is 20%. However, as the percentage of Ga in the material increases, up to 25%, magnetostriction decreases. This decline can be attributed to the organisation that manifests itself as the $D0_3$ structure. The results indicates the prepared Fe-Ga alloys will be useful for several real life applications.

Acknowledgement

The authors would like to express their gratitude to the Defence Metallurgical Research Laboratory (DMRL), Hyderabad for supporting this research.

References

1 Chen Y, Wang J, Yang B, Liu J & Jiang C, *J Al Com*, 856 (2021) 158166.
2 Golovin I S, Palacheva V V, Mohamed A K, Cifre J, Dubov L Y, Samoylova N Y & Balagurov A M, *J Al Com*, 864 (2021) 158819.
3 Adelani M O, Olive-Méndez S F, Espinosa-Magaña F, Matutes-Aquino J A & Grijalva-Castillo M C, *J Al Com*, 857 (2021) 157540.
4 Vijayanarayanan V, Banu R S, Kumar R S, Aravindhan V & Mahendran M, *AIP Conf Proc*, 2265 (2020).
5 Clark A E, Wun-Fogle M, Restorff J B, Lograsso T A & Cullen J R, *IEEE Trans Mag*, 37 (2001) 2678.
6 Lograsso T A, Ross A R, Schlagel D L, Clark A E & Wun-Fogle M, *J Al Com*, 350 (2003) 95.
7 Clark A E, Hathaway K B, Wun M, *J Appl Phys*, 93 (2003) 8621.
8 Li J, Xiao X, Yuan C, Gao X & Bao X, *J Rare Earths*, 33 (2015) 1087.
9 Jiang L, Zhang G, Jiandong Y, Hongbo H A O, Shangxia W U & Zengqi Z, *J Rare Earths*, 28 (2010) 409.
10 Taheri P, Barua R, Hsu J, Zamanpour M, Chen Y & Harris V G, *J Al Com*, 661 (2016) 306.
11 Elliott R, Magnetic Properties of Rare Earth Metals, Springer Science & Business Media, (2013).
12 Muralikrishna G M, Tas B, Esakkiraja N, Esin V A, Kumar K C H, Golovin I S, Belova I V, Murch G E, Paul A & Divinski S V, *Acta Materialia*, 203 (2021).
13 Palacheva V V, Emdadi A, Emeis F, Bobrikov I A, Balagurov A M , Divinski S V, Wilde G & Golovin I S, *Acta Materialia*, 130 (2017) 229.
14 Mohamed A K, Palacheva V V, Cheverikin V V, Zanaeva E N, Cheng W C, Kulitckii V, Divinski S, Wilde G & Golovin I S, *J Al Com*, 846 (2020) 156486.
15 Vijayanarayanan V, Basumatary H, Raja M M, Aravindan V, Sarathkumar R & Mahendran M, *Mater Today Proc*, 59 (2022) 216.
16 Vijayanarayanan V, Basumatary H, Raja M M, Aravindan V & Mahendran M, *ECS Trans*, 107 (2022) 17493.
17 Datta S, Huang M, Raim J, Lograsso T A, Flatau A B, *Mat Sci Eng A*, 435 (2006) 221.
18 Bhattacharyya S, Jinschek J R, Li J F & Viehland D, *J Al Com*, 501 (2010) 148.
19 Nivedita L R, Manivel P, Pandian R, Murugesan S, Morley N A, Asokan K & Kumar R T R, *J Magn Magn Mater*, 451 (2018) 300.
20 Dahal J, Ali K & Mishra S & J Alam, *Magnetochemistry*, 4 (2018) 54.
21 Xing Q, Du Y, McQueeney R J & Lograsso T A, *Acta Materialia*, 56 (2008) 4536.
22 Quinn C J, University of Salford (United Kingdom) (2012).
23 Cullen J R, Clark A E, Wun-Fogle M, Restorff J B & Lograsso T A, *J Magn Magn Mater*, 226 (2001) 948.
24 Golovin I S, Palacheva V V, Mohamed A K, Balagurov A M, *Phys Met Metallography*, 121 (2020) 851.

25 Emdadi A, Palacheva V, Cheverikin V, Churyumov A Y & Golovin I S, *J Magn Magn Mater*, 497 (2020) 165987.
26 Wang X, Liu Y, Chen X, Zhang H & Li Y, *China Foundry*, 17 (2020) 198.
27 Fitchorov T I, Bennett S, Jiang L, Zhang G, Zhao Z, Chen Y & Harris V G, *Acta Materialia*, 73 (2014) 19.
28 Gou J, Ma T, Liu X, Zhang C, Sun L, Sun G, Xia W & Ren X, *NPG Asia Mater*, 13 (2021).
29 Gao X, Li J, Zhu J, Li J & Zhang M, *Mat Trans*, 50 (2009) 1959.
30 Lin Y C, Lin C F, *J Appl Phys*, 117 (2015) 4.
31 Gao F, Jiang C, Liu J & Xu H, *J Appl Phys*, 100 (2006).
32 Perduta K, Olszewski J, Busbridge S & Nabiałek M, *Acta Phys Polonica A*, 114 (2008) 1537.
33 Turtelli R S, Bormio-Numes C, Sinnecker J P & Grössinger R, *Physica B: Con Mat*, 384 (2006) 265.
34 Bormio-Nunes C, Turtelli R S, Mueller H, Grössinger R, Sassik H, Tirelli M A, *J Magn Magn Mater*, 290-291 PA (2005) 820.
35 Lin Y C, *J Appl Phys*, 113 (2013) 17.
36 Sun A, Liu J & Jiang C, *Mater Des*, 88 (2015) 1342.